Effect of oxomolybdate species dispersion on direct methanol oxidation to dimethoxymethane over MoO x/TiO2catalysts

J. Faye, Mickaël Capron, A. Takahashi, Sébastien Paul, Benjamin Katryniok, T. Fujitani, Franck Dumeignil

Energy Science & Engineering

Open Access

RESEARCH ARTICLE

Effect of oxomolybdate species dispersion on direct methanol oxidation to dimethoxymethane over MoO_x/TiO_2 catalysts

Jérémy Faye[1], Mickaël Capron[2,3,4], Atsushi Takahashi[1], Sébastien Paul[3,5], Benjamin Katryniok[3,5], Tadahiro Fujitani[1] & Franck Dumeignil[2,3,4,6]

[1]Research Institute for Innovation in Sustainable Chemistry, AIST, Tsukuba West, Japan
[2]University of Lille Nord de France, F-59000 Lille, France
[3]Unité de Catalyse et de Chimie du Solide, UCCS (UMR CNRS 8181), F-59650, Villeneuve d'Ascq, France
[4]Université Lille 1 Sciences et Technologies, USTL, F-59652 Villeneuve d'Ascq, France
[5]Ecole Centrale de Lille, F-59655 Villeneuve d'Ascq, France
[6]Institut Universitaire de France, Maison des Universités, 103 Bd St-Michel, 75005 Paris, France

Keywords
Catalyst, dimethoxymethane, methanol, molybdenum, oxidation, titania

Correspondence
Jérémy Faye, Research Institute for Innovation in Sustainable Chemistry, AIST, Tsukuba West, Japan. E-mail: jeremy.faye@gmail.com
Franck Dumeignil, Univ. Lille Nord de France, F-59000, Lille, France. Tel: +33 (0) 3.20.33.49.49; Fax: +33 (0) 3.20.43.65.61; E-mail: franck.dumeignil@univ-lille1.fr

Funding Information
The authors would like to particularly acknowledge the National Institute for Advanced and Industrial Science of Technology, AIST, of Tsukuba West for supplying equipment, consumables and for taking in charge personal costs, together with the financial support of the International Research Group 'ECSAW' (Environmental Catalysis for Sustaining Clean Air and Water), between CNRS and AIST.

Received: 25 June 2014; Revised: 20 October 2014; Accepted: 26 November 2014

***Energy Science and Engineering* 2015, 3(2): 115–125**

doi: 10.1002/ese3.53

Abstract

The one-step selective oxidation of methanol to dimethoxymethane (DMM) was demonstrated over titania-supported molybdenum oxide catalysts, containing different amounts of molybdenum and prepared using two different impregnation techniques, namely wet impregnation and incipient wetness impregnation. The corresponding catalysts exhibited both acidic and redox properties, which are necessary for the oxidation of methanol to formaldehyde with subsequent condensation of the latter with excess methanol to finally yield DMM. The formation of well-dispersed polyoxomolybdate species on the catalyst surface was evidenced using IR-Raman, X-ray diffraction, and nitrogen physisorption. Varying the amount of these polyoxomolybdate species was associated with a modulation of the acidic and redox properties, as shown by NH_3-TPD and H_2-TPR. With respect to the catalytic performances, the best balance between acid and redox properties was observed over the samples containing 8 wt.% Mo, which corresponds to a theoretical MoO_x species coverage close to a monolayer.

Introduction

Dimethoxymethane (DMM) is a versatile molecule, which exhibits specific properties due to its C-O-C bonds that allow its use in various fields. For instance, it finds applications as a starting material in pharmaceutical and perfume industries or as a diesel fuel additive precursor (to synthesize polyoxymethylene dimethylether), which helps

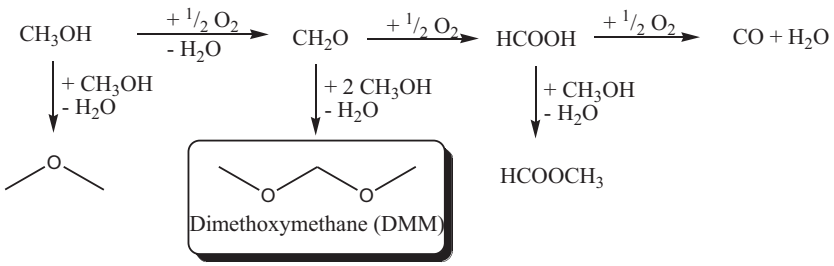

Scheme 1. Main and side reactions for the selective oxidation of methanol to dimethoxymethane (DMM).

reducing the particles emissions [1]. The current DMM production method is based on a two-step process: first, selective gas phase oxidation of methanol to formaldehyde (FA) is performed over an iron molybdate catalyst, and the so-obtained FA is then reacted with methanol in a second reactor to form DMM over acid catalysts, either in the liquid or the gas phase (Scheme 1) [2].

With regard to investment costs and safety issues (FA being classified as a Carcinogenic, Mutagenic, Reprotoxic (CMR) substance), the selective one-pot oxidation of methanol to DMM would be highly preferred compared to the aforementioned two steps process. Thus, a bifunctional catalyst is required, which must contain both acid and redox properties, in order to promote both the oxidation to FA and its subsequent condensation with methanol (Scheme 1). Numerous research articles addressed the development of new catalysts for this reaction, whereby generally four types of catalysts were described based either on supported vanadium [3–10], ruthenium [11, 12], rhenium [13–17] or molybdenum [10, 18–21]. Regarding the fine-tuning of the redox and the acid properties, several strategies can be employed. For example, Liu et al. used a Keggin-type vanado-phosphomolybdic acid heteropolycompound which is a well-known acid and redox catalyst [22, 23]. Other researchers doped vanadium-based catalysts with sulfate or phosphate ions in order to increase their acid character [24–26]. Nevertheless, the most widely spread out technique is the use of an acidic support, such as niobium phosphate [27], alumina [28], zirconia [29] or – most frequently – titania [9, 30–32], as a carrier for the metal oxide compound bringing redox properties, of which the dispersion on the support further influences its acidity (notably by modifying the number of bare accessible acid sites) and thus the catalytic performances. More recently, Kaichev et al. claimed that a titania-supported geometric monolayer of vanadium oxide shows good catalytic performance for the selective oxidation of methanol to DMM [33]. With regard to these results, we decided to study the influence of the dispersion for another well-established model catalyst [34] polyoxomolybdate supported on titania.

Experimental

Synthesis

Titania-supported polyoxomolybdate catalysts were prepared either by the wet impregnation (WI) or by the incipient wetness impregnation (IWI) technique. The amount of molybdenum was varied between 1 and 14 wt.% by dispersion on the support. Correspondingly, the catalysts were labeled *X*Mo(IWI) or *X*Mo(WI) according to the preparation technique and the amount of molybdenum (*X*) in weight percent.

The synthesis of catalysts by WI was conducted as follows: ammonium heptamolybdate tetrahydrate ($[NH_4]_6Mo_7O_{24}{\cdot}4H_2O$; Wako Pure Chemical Industries, Ltd., Osaka, Japan) was slowly added to a fixed volume of water (50 cm^3), stirred at room temperature until complete dissolution, and the titania support (Hombikat F01; Sachtleben Chemie GmbH, Duisburg, Germany) was finally poured under stirring. The respective amounts of ammonium heptamolybdate and support were adjusted in order to obtain the desired loading of molybdate on titania. The suspension was heated up to 50°C, and the excess of solvent was evaporated at this temperature under reduced pressure. The obtained solid was dried at 110°C overnight before being calcined at 500°C for 3 h (heating rate: 1.5°C min^{-1}).

Due to the solubility limit of the molybdenum precursor ($[NH_4]_6Mo_7O_{24}{\cdot}4H_2O$) in water and to the pore volume of the support, the Mo loading was technically limited to 8 wt.% for samples prepared by the IWI procedure. A typical synthesis was carried out as follows: after determining the pore volume of the titania support with water (*ca.* 0.3 $cm^3\ g^{-1}$), the required volume of ammonium heptamolybdate tetrahydrate solution was slowly added to the titania support (Hombikat F01; Sachtleben) in an agate mortar under grinding in order to prepare 1 g of catalyst. When the addition was completed, the obtained solid was dried at 100°C overnight before being calcined at 500°C for 3 h (heating rate: 1.5°C min^{-1}).

Characterizations

The surface area and the total pore volume of the catalysts were determined using nitrogen physisorption/desorption technique at the temperature of liquid nitrogen (ASAP 2010; Micromeritics Instrument Corporation, Norcross, GA). The specific surface area (SSA) was calculated using the BET method, and the pore volume (Vp) was determined using the point recorded at the relative pressure $P/P_0 = 0.995$. Before analysis, the samples were outgassed at 120°C for 3 h under vacuum.

Raman spectroscopy was performed on a LabRam Infinity apparatus (Horiba Jobin-Yvon, Kyoto, Japan) equipped with a CCD detector operating at liquid nitrogen temperature. The samples were excited by a He–Ne laser at 632.81 nm. The Raman shift was recorded in the 200–1600 cm^{-1} range.

The structure of the catalysts was analyzed by X-ray diffraction (XRD) on a Rigaku RINT-2000 diffractometer, using the CuKα radiation ($\lambda = 1.5418$ Å) as an X-ray source. Patterns were recorded between 20 and 90° (2θ), with a step fixed at 0.04° and a scan speed of 1.5°min^{-1}.

The reducibility of the catalysts was evaluated using a Bel-cat device by temperature-programmed reduction (H_2-TPR). Therefore, 100 mg of freshly calcined catalyst was loaded in a quartz reactor and pretreated in a He flow (30 cm^3 min^{-1}) at 500°C for 2 h. Then, helium was replaced by a gas mixture containing 5 mol.% of hydrogen in helium. The temperature of the reactor was increased from 100 to 800°C at a rate of 10°C min. The effluent gas was analyzed by a thermal conductivity detector (TCD).

The acidity of the catalysts was evaluated using temperature-programmed desorption of ammonia (NH_3-TPD). Prior to adsorption, the samples were pretreated at 500°C in order to remove any water or adsorbed contaminant trace. Then, the samples were cooled to 100°C, and ammonia was subsequently absorbed using pulsed injections until saturation was observed from the TCD signal. The TPD profiles were monitored by a TCD and recorded from 100 to 600°C at a heating rate of 10°C min.

Methanol oxidation reaction

The catalytic activity in the reaction of selective oxidation of methanol was determined in a fixed bed down-flow reactor working at atmospheric pressure. The catalytic tests were performed with 50 mg of catalyst sieved between 14 and 22 mesh. Prior to the catalytic reaction, each catalyst was activated under pure oxygen at 300°C (final reaction temperature) during 1 h. Methanol was evaporated by bubbling the O_2/He gas flow in liquid methanol (99.99%, Wako) at 35°C and further condensed at 11°C in order to obtain a constant methanol partial pressure of 7680 Pa. Thus, the final reaction mixture was composed of 7.5/15.5/77 vol. % for methanol/oxygen/helium at a gas hourly space velocity of 26 L h^{-1} g_{cat}^{-1} STP. The reaction temperature was stepwise (each 10°C) varied between 100 and 300°C. The products were analyzed by an online analytical system composed of sampling loops enabling simultaneous injection of the reactor outlet gas mixture in two Shimadzu GC-14B gas phase chromatographs. A packed Porapak T column ($L = 2$ m, $ID = 3$ mm) with TCD detection was employed to separate and quantify FA, dimethylether, water, methanol, methyl formate, and DMM, while permanent gases (O_2, CO and CO_2) were preseparated from organic compounds using a Porapak Q column ($L = 2$ m; $ID = 3$ mm), further separated on a Shincarbon ST column ($L = 2$ m; $ID = 3$ mm) and quantified with a TCD.

Table 1. Textural parameters of the prepared catalysts.

Sample	SSA (m^2 g^{-1})	Pore volume (cm^3 g^{-1})	Average pore size diameter (nm)	Theoretical number of layers [36]
Parent TiO_2	107	0.30	5.2	–
1Mo(IWI)	114	0.30	4.5	0.09
2Mo(IWI)	118	0.31	4.5	0.18
4Mo(IWI)	122	0.28	4.0	0.36
8Mo(IWI)	145	0.25	3.3	0.72
1Mo(WI)	110	0.29	5.3	0.09
2Mo(WI)	118	0.30	4.5	0.18
4Mo(WI)	122	0.29	4.6	0.36
8Mo(WI)	154	0.29	3.6	0.72
12Mo(WI)	172	0.28	3.2	1.08
14Mo(WI)	171	0.24	3.3	1.27

SSA, specific surface area.

Results and Discussion

Characterization

The supports and catalysts were characterized using various techniques in order to evaluate their physical and chemical properties. First, the textural properties were studied, notably to determine the pore volume, which is, for example, a key parameter for the IWI method.

The parent commercial titania support exhibited a SSA of 107 m^2 g^{-1} with a total pore volume of 0.30 cm^3 g^{-1} (Table 1). Correspondingly, the preparation method for the IWI was elaborated using 3 cm^3 of molybdate solution for 10 g of titania support. It is further noteworthy that the average pore diameter of the parent titania is

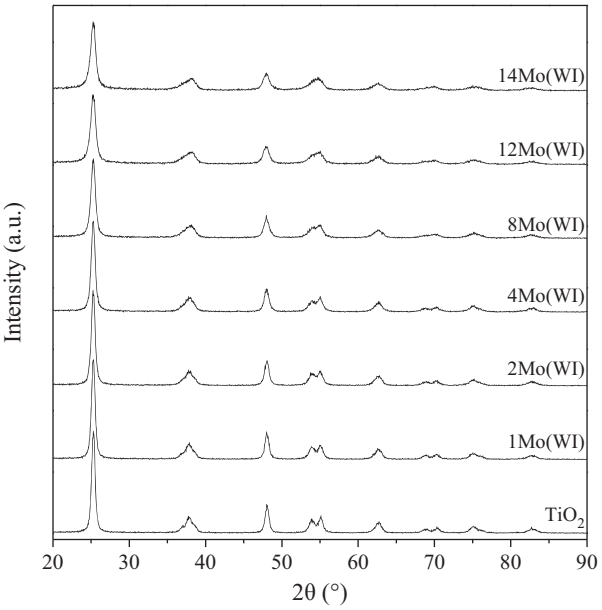

Figure 1. X-ray diffraction (XRD) patterns for the catalyst prepared by the wet impregnation method.

5.2 nm with a narrow pore size distribution (Fig. S1). Upon impregnation with molybdenum, two trends can be observed: whereas the SSA increases with the amount of impregnated molybdenum, the pore volume and the average pore diameter decrease (Table 1). This behavior is observed for both types of impregnation techniques at the same extent with, for example, comparable SSA s at iso-Mo content, which suggests the formation of a microporous network exhibiting a high surface area, as observed on the nitrogen adsorption–desorption curves and pore size distribution plots (Fig. S2). This general trend for a decrease in pore volume and pore diameter was ascribed to the formation of polyoxomolybdate species in the porous network of the support, thus coating the pores.

The geometrical monolayer coverage was calculated assuming the formation of MoO_3 species according to an occupancy of 15.4 $Å^2$ [35] and, obviously, to the SSA of the support. The results showed that the impregnation on the high surface titania enabled the synthesis catalysts with coverage varying from 0.09 monolayers (1 wt.% Mo) up to 1.26 monolayers (14 wt.% Mo) (Table 1, [36]). Consequently, the samples exhibiting the highest coverage without exceeding the monolayer are, in this study, the two 8 wt.% Mo solids, while 12Mo(WI) can be considered as representative of a sample covered with a MoO_x species monolayer (only slightly overloaded, with a theoretical number of monolayers of 1.08).

The structural features of the catalysts were determined by XRD and IR-Raman spectroscopy. The XRD patterns (Figs. 1 and S3) confirm that the employed titania is of the anatase type (JCPDS 84-1286) with characteristic 2θ diffraction peaks at 25° (101), 37–38° (103; 004; 112), 48° (200), 54° (105), 55° (211), and 63° (118). Upon impregnation with molybdenum, no significant change can be observed, irrespective of the impregnation method or the amount of Mo. The formation of crystallized molybdenum-VI-oxide (MoO_3) can completely be ruled out since its main diffraction peak at $2\theta = 25°$ was absent, which was also the case for the second most intense peak at 39°. Hence, three hypotheses can be formulated: (1) Crystalline MoO_3 was formed, but in a quantity below the XRD detection limit, (2) an amorphous phase of molybdate was formed, or (3) a nano-crystalline phase was formed, with a crystal size under the XRD detection limit.

Next, IR-Raman was employed to precisely determine the nature of the molybdenum phase. The full-scale spectra (Figs. 2 left and S4) are dominated by the three characteristic Raman peaks of titania at 393, 515, and 638 cm^{-1}. Additional Raman bands were observed from 2 wt.% Mo with a peak at *ca.* 938 cm^{-1} that progressively shifted to higher wavenumbers (up to *ca.* 965 cm^{-1}) when increasing the Mo loading (Figs. 2 right and S5), accompanied with a slight shoulder at 840 cm^{-1}. With respect to the literature, the corresponding signals can be ascribed to isolated monomeric molybdates species at low loadings and to polyoxomolybdate species for higher Mo coverage extents (vide infra) [37–41]. Again, in agreement with the XRD patterns, we could clearly and definitely rule out the formation of the MoO_3 phase (characteristic intense Raman band that should arise at 825 cm^{-1}).

After the physical properties, the chemical properties (acidity and reducibility) were determined by temperature-programmed desorption of ammonia and by temperature-programmed reduction, respectively, for both series of catalysts. These two parameters are crucial for the catalytic performance, since the selective oxidation of methanol to DMM requires a bifunctional catalyst combining acidity and redox characters. The results will be presented for solids prepared by WI, since very similar properties in terms of texture, crystalline structure and catalytic behavior were obtained using both synthesis procedures.

The temperature-programmed desorption of ammonia (Fig. 3 and Table 2) showed that the ammonia uptake decreased when increasing the amount of impregnated Mo species. This can be ascribed to the progressive coverage of the acid sites of the titania support by polyoxomolybdate species. As shown in Figure 3B, it is notably noteworthy that the strong acid sites (with a NH_3 desorption temperature comprised between 300 and 550°C) are covered first. Hence, the ammonia uptake dropped from 620 μmol g^{-1} (bare support) to 409 μmol g^{-1} upon impregnation with 1 wt.% molybdenum (Fig. 3B). Further addition of molybdenum only slightly decreased the

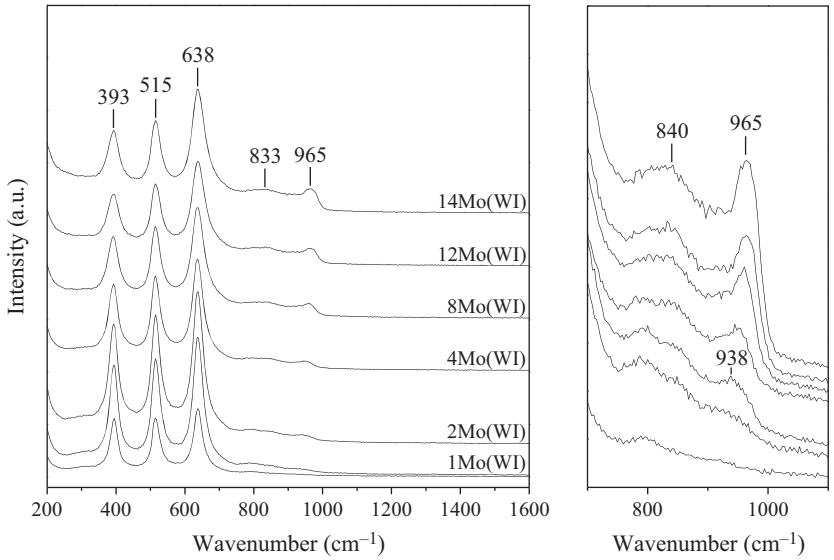

Figure 2. Raman spectra of the catalysts prepared by the wet impregnation method (left: full scale, right: 700–1100 cm^{-1} zone).

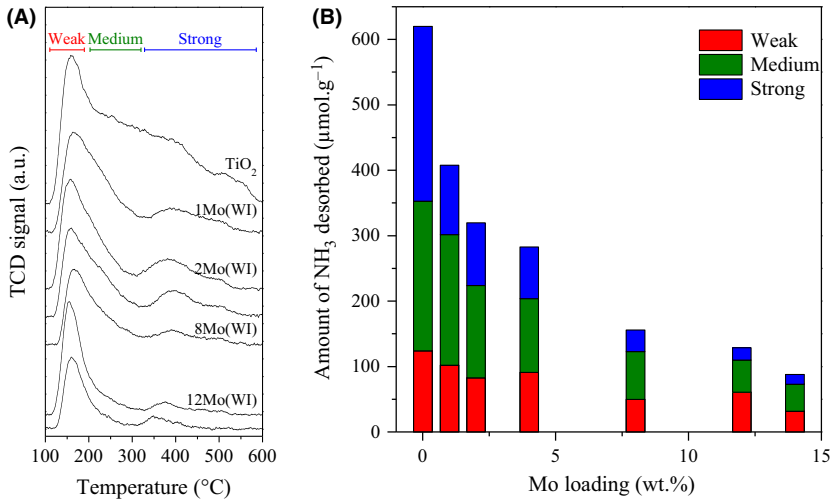

Figure 3. (A) Temperature-programmed desorption of ammonia for the catalyst prepared by the wet impregnation technique; (B) Ammonium uptake as a function of the molybdenum loading.

amount of acid sites, whereby a roughly linear trend between the NH_3 uptake and the Mo amount can be observed from 1 to 14 wt.% Mo (Fig. 3 and Table 2). Thus, the impregnation with molybdenum affected the remaining weak and medium acid sites (ammonia desorption temperature 130–350°C) by progressively covering them. Further, as the measures are given for one gram of catalyst, the amount of titania itself mechanically decreases corresponding to the impregnated quantity of molybdenum. Thus, the decrease in the number of acid sites is not only due to an increase in the surface coverage extent but also to the quantity of TiO_2 effectively present in each sample. Finally, the fact that some acidic properties still remain after the theoretical monolayer coverage is reached, namely for 12Mo(WI) and 14Mo(WI) (see Table 1), suggests that a perfect bidimensional monolayer is not achieved with some Mo species stacking and/or that the introduction of Mo species is responsible for the development of some acid properties. De Almeida et al. [42] and Shao et al. [43] recently reported the enhancement of their catalysts acidity when supporting molybdenum oxide on TiO_2 or mesoporous silica, respectively. The FT-IR study realized by Shao et al. after pyridine adsorption suggested that the formation of Si–O–Mo bonds helps in the development of the acidic character of the Mo species supported on SiO_2 solids. Thus, the oxo-

Table 2. Chemical parameters of the catalysts prepared by wet impregnation.

	TiO_2	1Mo(WI)	2Mo(WI)	4Mo(WI)	8Mo(WI)	12Mo(WI)	14Mo(WI)
NH_3 consumption ($\mu mol\ g^{-1}$)							
<300°C	353	299	227	198	118	107	71
Total	620	409	320	283	155	129	88
H_2 uptake ($\mu mol\ g^{-1}$)							
<300°C	0	0.3	0.2	0.7	0.7	0.7	0.5
Total	7.5	33.7	62.8	110.5	193.0	266.7	330.4

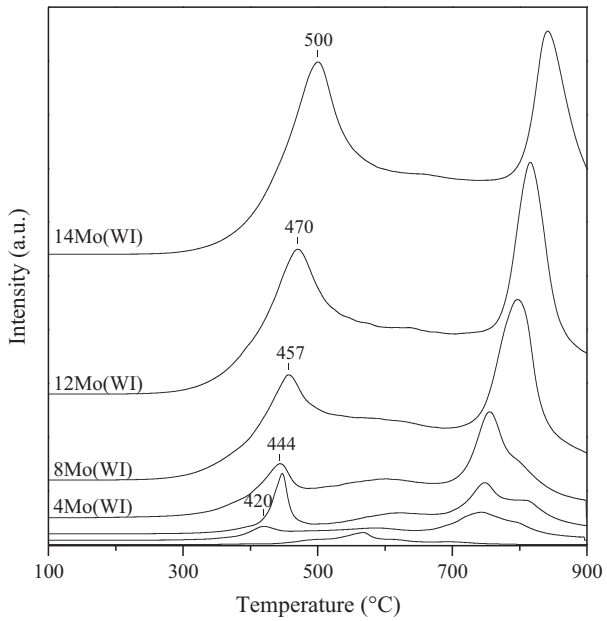

Figure 4. Profiles of the temperature-programmed reduction in the catalysts prepared by wet impregnation technique.

molybdate species supported on TiO_2 lead to a combined effect of decreased acidity of the support when increasing the Mo loading (by covering), and to the simultaneous creation of a new acidity through the formation of acid sites of a different nature with the creation of the Ti–O–Mo bonds.

The redox properties of the catalysts were then evaluated by thermoreduction using hydrogen as a reducing agent. The corresponding TPR profiles for the catalysts prepared by the WI technique are reported in Figure 4.

The parent TiO_2 support exhibited low reducibility (Fig. 4). However, even small addition of molybdenum significantly enhanced reducibility by increasing, with an increase in hydrogen consumption from 7.5 $\mu mol\ g^{-1}$ (bare TiO_2, Table 2) to 33.7 $\mu mol\ g^{-1}$ (1Mo(WI), Table 2). As expected, the total hydrogen consumption increased with the amount of molybdenum in the catalyst (Table 2), due to the well-know partial reduction in Mo^{6+} to Mo^{4+} over this kind of systems [44]. Furthermore, an increase in the reduction temperature was observed for higher loadings of Mo, in agreement with similar catalytic systems reported in the literature [45]. In fact, whereas the catalyst containing 1 wt.% Mo exhibited the maximum of the reduction peak at 420°C, this maximum was shifted to 457°C for the catalyst with 8 wt.% Mo, and even to 500°C for the catalyst containing 14 wt.% Mo. The lower reduction temperature for the low loadings suggests that the polyoxomolybdate phase is very well dispersed, whereby the reduction is facilitated. Finally, the second hydrogen consumption peak above 700°C corresponds to the complete reduction in molybdenum [44].

Regarding the experimental conditions for the determination of the catalytic activities in methanol conversion, a calculation of the hydrogen consumption up to 300°C was realized to be consistent with the catalysis operating conditions. Note that, in a previous work, we observed that the reduction with H_2 and the reduction with methanol gave exactly the same results over a FeMo catalyst used for direct methanol conversion, whereby hydrogen is an appropriate probe molecule well representing the reduction with methanol [18]. The results presented in Table 2 indicate that, despite a global increase in H_2 with the Mo loading, the hydrogen consumption at 300°C showed an maximum for the 8Mo(WI) sample (0.7 $\mu mol\ g^{-1}$) and decreased for higher Mo contents. This suggests that the solid containing 8 wt.% in molybdenum exhibits the most appropriate reduction properties in the range of the reaction temperature (100–300°C, vide infra).

Catalytic performances

The catalytic performances of the samples containing different amounts of molybdenum and prepared by both impregnation techniques were evaluated in the selective oxidation of methanol at different temperatures. Thus, typical light-off curves were obtained (Fig. 5).

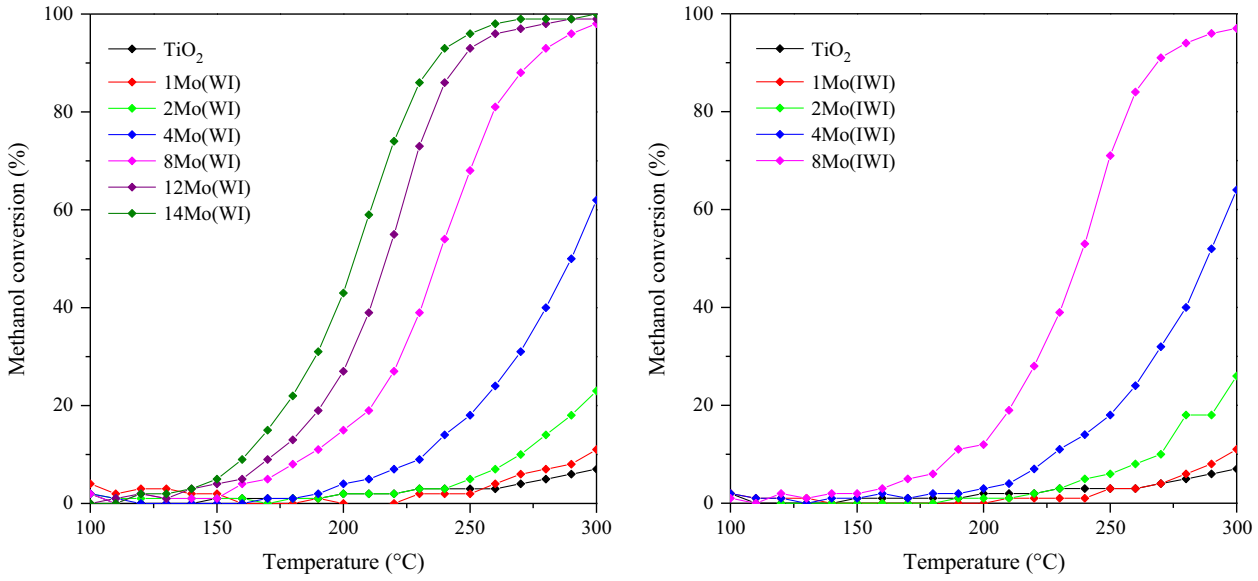

Figure 5. Conversion of methanol over the catalysts prepared by wet impregnation (left) and incipient wetness impregnation (right).

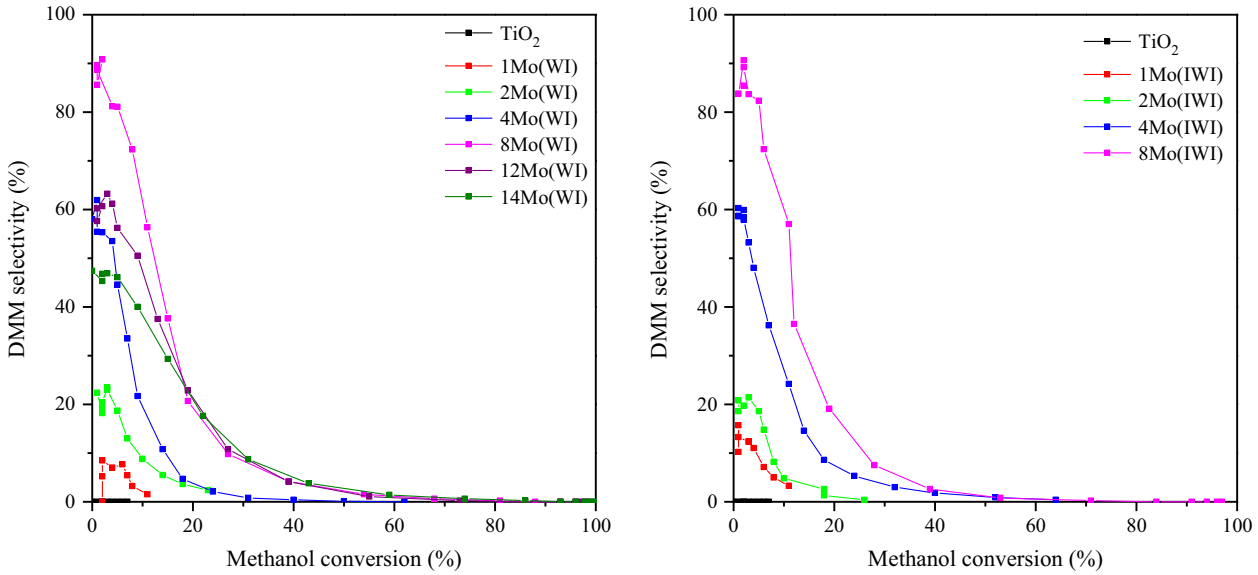

Figure 6. Selectivity to dimethoxymethane (DMM) over the catalysts prepared by wet impregnation (left) and incipient wetness impregnation (right) as a function of methanol conversion.

The catalytic activity increased with the amount of molybdenum. In fact, whereas the catalyst without molybdenum shows nearly no catalytic activity (less than 10% conversion at 300°C), the catalyst containing 4 wt.% molybdenum exhibits 64% conversion at 300°C. For higher molybdenum loadings of 8, 12, and 14 wt.%, full conversion is obtained at 300, 275, and 270°C, respectively. It is noteworthy that the preparation method (WI or IWI), had almost no impact on the catalytic activity (i.e., both catalysts containing 4 wt.% Mo, show identical conversion in the 200–300°C range), suggesting thus that the dispersion of the polyoxomolybdate phase was identical for both preparation methods, which is in agreement with the previous characterization results (BET, Raman, XRD). Moreover, this phenomenon is consistent with the results reported by Knözinger and Taglauer [46, 47] in their reviews on wetting and spreading. Indeed, these authors deeply investigated the preparation of supported metals or supported oxides from thermodynamic and experimental points of view, especially comparing the

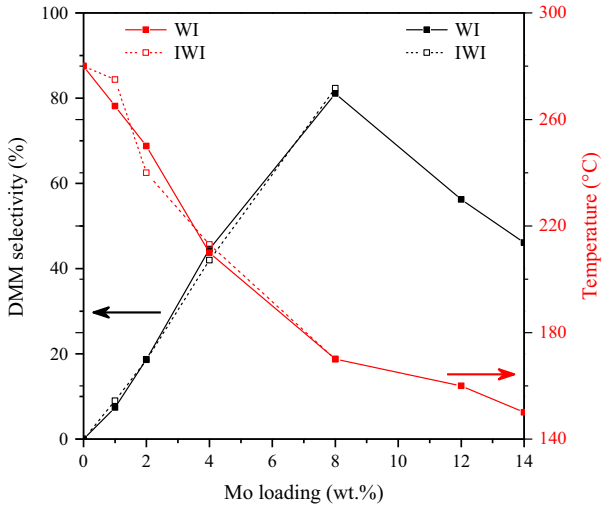

Figure 7. Reaction temperature required for 5% conversion of methanol and corresponding selectivity to DMM.

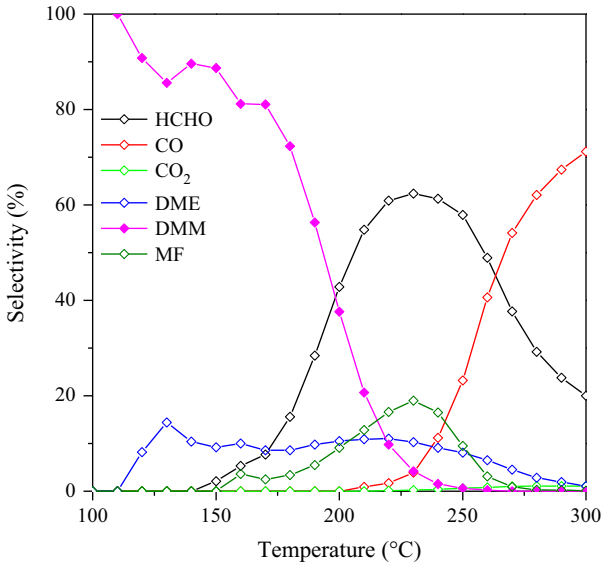

Figure 8. Selectivity over the 8Mo(WI) catalyst as function of the reaction temperature.

results obtained by numerous authors for MoO_x/TiO_2 prepared by physical mixture of MoO_3 and TiO_2 followed by calcination. The differences in surface free energies of TiO_2 and MoO_3 largely favor the spreading of molybdate species on the surface of the support through the formation of interfacial $Ti(MoO_4)_2$, which strongly supports the observations made in this work of high dispersion of molybdate species, even if the detection of the $Ti(MoO_4)_2$ was certainly not evidenced due to its low content. Moreover, authors indicated that the presence of water vapor increases the rate of spreading, leading to monomeric surface molybdate MoO_4^{2-} species (with a characteristic Raman band at 915 cm^{-1}) that further condense to form polymolybdate species (950 cm^{-1}) according to the Mo loading. When using preparation methods based on WI or IWI, the formation of molybdate surface species of different polymerization extents was evidenced by Raman spectroscopy as depicted in Figure 2 with the progressive shift of the molybdates band to higher wave numbers.

Concerning the products formation, the increase in molybdenum content promoted the selective formation of DMM for amounts up to 8 wt.%. The results are presented in Figure 6 that plots the selectivities to DMM versus methanol conversion, similarly to the results reported by Sun et al. [48].

This compound was notably formed with high selectivity for low methanol conversions (<20%), showing up to 90% selectivity to DMM (at 5% in methanol conversion) for the catalysts with 8 wt.% Mo. In fact, at low conversion, the intermediately formed FA remains adsorbed to the surface of the catalysts, whereby it remains accessible for the further condensation reaction to DMM. On the other hand, at high methanol conversion rate, the adsorption equilibrium of FA is shifted to the desorbed species, whereby the successive reaction to DMM decreases with temperature.

The fact that the preparation technique had no influence on the catalytic performance was further confirmed by experiments at iso-conversion of methanol (5%). The required reaction temperature for obtaining 5% conversion of methanol, and the selectivity in DMM depended only on the amount of molybdenum, but not on the employed impregnation technique (Fig. 7).

From these results, one can further see that the increase to 12 wt.% and 14 wt.% Mo resulted in a decreased selectivity to DMM, thus meaning that the catalysts with 8 wt.% Mo showed the best performance in the selective oxidation of methanol to DMM. These results are in agreement with the previous TPR results already suggesting that the 8Mo(WI) exhibits the largest reducibility under reaction conditions. Concerning the influence of the coverage, it is noteworthy that Kaichev et al. [33] reported that a vanadium-V-oxide monolayer was favorable, whereas we found that a submonolayer of polyoxomolybdate was the optimum. This can be explained by the different redox-potentials of molybdenum and vanadium, leading thus to different optimum amounts for the fine-tuning of the acid-redox properties.

Concerning the product distribution over the 8Mo(WI) catalyst, DMM was the main product for a reaction temperature below 200°C. Afterward, the formation of FA was strongly promoted up to 260°C (Fig. 8) before finally carbon monoxide became the main product (>260°C).

Thus, one can conclude that the oxidation of methanol over the redox sites becomes predominant over the con-

densation to DMM for increased temperature, leading to oxidation products such as carbon monoxide. This is also supported by the decrease in the formation of dimethylether, which is also formed by condensation of methanol over acid sites. Nevertheless, even for increased reaction temperature, the carbon balance always remained higher than 90% (Fig. S6). Hence, the optimum balance between the redox reaction rate and the condensation reaction rate is obtained for the 8Mo(WI) catalyst at 190°C. However, by comparison with vanadia–titania catalytic systems, it appears that MoO_x remained less active that VO_x since authors like Sun et al. [48] reported the preparation of 10 wt.% V_2O_5 on TiO_2 that allowed converting 26% of methanol with 95% of selectivity to DMM at 160°C. Lu et al. [25] determined the chemical properties by H_2-TPR and NH_3-TPD to assess the reducibility and the acidity, respectively, of their V_2O_5/TiO_2 solids. Redox properties results showed a hydrogen consumption peak located around 500°C, accompanied with a peak broadening when increasing the amount of vanadium. This result is quite similar to the H_2-TPR results obtained for MoO_x/TiO_2 since the main hydrogen consumption peak is located in the same temperature range, that is, 450–500°C. However, the oxidation states in these two catalytic systems are different: (+6) for molybdenum and (+5) for vanadium, and the reduction processes are different. Taking into account this property, it is quite difficult to differentiate those two catalysts even if we can mention that MoO_x is probably more reducible since the oxidation state of Mo is higher. On the other hand, differences appear from the acidity point of view. Indeed, Lu et al. [25] showed that an increase in vanadium loading leads to a decrease in surface acidity, especially for weak Brønsted acid sites (located around 200°C), while in our case, the increase in Mo loading seems to affect the medium and strong acidic sites (Fig. 3). Guo et al. [26, 30] provided a quantitative estimation of the global acidity of their vanadia–titania catalyst: even if the titania used to prepare the MoO_x/TiO_2 in our work exhibits a high global acidity (620 μmol g^{-1} vs. 374.2 μmol g^{-1}), the addition of Mo significantly affected the surface acidity (88 μmol g^{-1} for the 14Mo(WI)), whereas the acidity of the V_2O_5–TiO_2 catalysts of Guo et al. [30] increased to 30 wt.% in V_2O_5. As a conclusion, the nature of the active phase and also the nature of the parent support seem to have an influence of the activity, especially linked with surface acid properties.

Conclusion

The selective catalytic oxidation of methanol to DMM was studied over titania-supported polyoxomolybdate catalysts prepared using different amounts of molybdenum impregnated either by IWI or by WI to force the deposition of higher loadings. From the characterization using XRD, Raman and nitrogen physisorption, we identified molybdate species forming a submonolayer of polyoxomolybdates when the Mo loading increased. Comparing the two impregnation techniques, no difference was found neither in physical and chemical properties, nor in the catalytic performance, with a good dispersion of molybdenum species obtained by both techniques. From the catalytic results, it becomes further clear that the optimum amount of molybdenum was 8 wt.%, which corresponded to a submonolayer of polyoxomolybdate and exhibits the best redox-character within the range of the reaction temperature as well as balanced acidity.

Conflict of Interest

None declared.

References

1. Ball, J. C., C. Lapin, J. Buckingham, E. Frame, D. Yost, J. Garbak, et al. 2001. Dimethoxy methane in diesel fuel: part 1. the effect of fuels and engine operating modes on emissions of toxic air pollutants and gas/solid phase PAH.
2. Soares, A. P. V., M. F. Portela, and A. Kiennemann. 2005. Methanol selective oxidation to formaldehyde over iron molybdate catalysts. Catal. Rev. 47:125–174.
3. Liu, J., Q. Sun, Y. Fu, and J. Shen. 2009. Preparation and characterization of mesoporous VO_x-TiO_2 complex oxides for the selective oxidation of methanol to dimethoxymethane. J. Colloid Interface Sci. 335:216–221.
4. Zhao, H., S. Bennici, J. Shen, and A. Auroux. 2009. Surface and catalytic properties of V_2O_5–TiO_2/SO_4^{2-} catalysts for the oxidation of methanol prepared by various methods. J. Mol. Catal. A Chem. 309:28–34.
5. Guo, H., D. Li, D. Jiang, W. Li, and Y. Sun. 2010. Characterization and performance of sulfated VO_x–TiO_2 catalysts in the one-step oxidation of methanol to dimethoxymethane. Catal. Commun. 11:396–400.
6. Zhao, H., S. Bennici, J. Shen, and A. Auroux. 2009. Calorimetric study of the acidic character of V_2O_5–TiO_2/SO_4^{2-} catalysts used in methanol oxidation to dimethoxymethane. J. Therm. Anal. Calorim. 99:843–847.
7. Guo, H., D. Li, D. Jiang, W. Li, and Y. Sun. 2010. The one-step oxidation of methanol to dimethoxymethane over nanostructure vanadium-based catalysts. Catal. Lett. 135:48–56.
8. Zhao, H., S. Bennici, J. Shen, and A. Auroux. 2010. Nature of surface sites of V_2O_5–TiO_2/SO_4^{2-} catalysts and reactivity in selective oxidation of methanol to dimethoxymethane. J. Catal. 272:176–189.

9. Zhao, H., S. Bennici, J. Cai, J. Shen, and A. Auroux. 2010. Effect of vanadia loading on the acidic, redox and catalytic properties of V_2O_5–TiO_2 and V_2O_5–TiO_2/SO_4^{2-} catalysts for partial oxidation of methanol. Catal. Today 152: 70–77.
10. Royer, S., X. Sécordel, M. Brandhorst, F. Dumeignil, S. Cristol, C. Dujardin, et al. 2008. Amorphous oxide as a novel efficient catalyst for direct selective oxidation of methanol to dimethoxymethane. Chem. Commun. 7:865–867.
11. Liu, H., and E. Iglesia. 2005. Selective oxidation of methanol and ethanol on supported ruthenium oxide clusters at low temperatures. J. Phys. Chem. B 109:2155–2163.
12. Yu, H., K. Zeng, X. Fu, Y. Zhang, F. Peng, H. Wang, et al. 2008. RuO_2 xH_2O supported on carbon nanotubes as a highly active catalyst for methanol oxidation. J. Phys. Chem. C 112:11875–11880.
13. Yuan, Y., H. Liu, H. Imoto, T. Shido, and Y. Iwasawa. 2000. Selective synthesis of methylal from methanol on a new crystalline $SbRe_2O_6$ catalyst. Chem. Lett. 29:674–675.
14. Yuan, Y., T. Shido, and Y. Iwasawa. 2000. The new catalytic property of supported rhenium oxides for selective oxidation of methanol to methylal. Chem. Commun. 15:1421–1422.
15. Yuan, Y., and Y. Iwasawa. 2002. Performance and characterization of supported rhenium oxide catalysts for selective oxidation of methanol to methylal. J. Phys. Chem. B 106:4441–4449.
16. Sécordel, X., A. Yoboué, S. Cristol, C. Lancelot, M. Capron, J.-F. Paul, et al. 2011. Supported oxorhenate catalysts prepared by thermal spreading of metal Re^0 for methanol conversion to methylal. J. Solid State Chem. 184:2806–2811.
17. Nikonova, O. A., M. Capron, G. Fang, J. Faye, A.-S. Mamede, L. Jalowiecki-Duhamel, et al. 2011. Novel approach to rhenium oxide catalysts for selective oxidation of methanol to DMM. J. Catal. 279:310–318.
18. Thavornprasert, K.-A., M. Capron, L. Jalowiecki-Duhamel, O. Gardoll, M. Trentesaux, A.-S. Mamede, et al. 2014. Highly productive iron molybdate mixed oxides and their relevant catalytic properties for direct synthesis of 1,1-dimethoxymethane from methanol. Appl. Catal. B 145:126–135.
19. Gornay, J., X. Sécordel, G. Tesquet, B. de Ménorval, S. Cristol, P. Fongarland, et al. 2010. Direct conversion of methanol into 1,1-dimethoxymethane: remarkably high productivity over an FeMo catalyst placed under unusual conditions. Green Chem. 12:1722–1725.
20. Gornay, J., X. Secordel, M. Capron, G. Tesquet, P. Fongarland, E. Payen, et al. 2010. Synthèse directe du 1,1-diméthoxyméthane à partir de méthanol moyennant une modification mineure du procédé de production de formaldéhyde sur catalyseurs FeMo. Oil Gas Sci. Technol. Rev. d'IFP Energies Nouv. 65:751–762.
21. Thavornprasert, K.-A., B. de la Goublaye de Ménorval, M. Capron, J. Gornay, L. Jalowiecki-Duhamel, X. Sécordel, et al. 2012. Selective oxidation of ethanol towards a highly valuable product over industrial and model catalysts. Biofuels 3:25–34.
22. Liu, H., and E. Iglesia. 2003. Selective one-step synthesis of dimethoxymethane via methanol or dimethyl ether oxidation on $H_{3+n}V_nMo_{12-n}PO_{40}$ Keggin structures. J. Phys. Chem. B 107:10840–10847.
23. Liu, H. 2004. Effects of support on bifunctional methanol oxidation pathways catalyzed by polyoxometallate Keggin clusters. J. Catal. 223:161–169.
24. Chen, S., S. Wang, X. Ma, and J. Gong. 2011. Selective oxidation of methanol to dimethoxymethane over bifunctional VO_x/TS-1 catalysts. Chem. Commun. 47:9345–9347.
25. Lu, X., Z. Qin, M. Dong, H. Zhu, G. Wang, Y. Zhao, et al. 2011. Selective oxidation of methanol to dimethoxymethane over acid-modified V_2O_5/TiO_2 catalysts. Fuel 90:1335–1339.
26. Guo, H., Y. Xiao, J. Wang, Z. Fan, D. Li, and Y. Sun. 2013. Influence of preparation method on the surface and catalytic properties of sulfated vanadia–titania catalysts for partial oxidation of methanol. Fuel Process. Technol. 106:77–83.
27. Sun, Q., D. Fang, S. Wang, J. Shen, and A. Auroux. 2007. Structural, acidic and redox properties of V_2O_5/NbP catalysts. Appl. Catal. A 327:218–225.
28. Sun, Q., A. Auroux, and J. Shen. 2006. Surface acidity of niobium phosphate and steam reforming of dimethoxymethane over $CuZnO/Al_2O_3$–NbP complex catalysts. J. Catal. 244:1–9.
29. Zhao, Y., Z. Qin, G. Wang, M. Dong, L. Huang, Z. Wu, et al. 2013. Catalytic performance of V_2O_5/ZrO_2–Al_2O_3 for methanol oxidation. Fuel 104:22–27.
30. Guo, H., D. Li, D. Jiang, H. Xiao, W. Li, and Y. Sun. 2010. Characterization and performance of V_2O_5–TiO_2 catalysts prepared by rapid combustion method. Catal. Today 158:439–445.
31. Fu, Y., and J. Shen. 2007. Selective oxidation of methanol to dimethoxymethane under mild conditions over V_2O_5/TiO_2 with enhanced surface acidity. Chem. Commun. 21:2172–2174.
32. Secordel, X., E. Berrier, M. Capron, S. Cristol, J.-F. Paul, M. Fournier, et al. 2010. TiO_2-supported rhenium oxide catalysts for methanol oxidation: effect of support texture on the structure and reactivity evidenced by an operando Raman study. Catal. Today 155:177–183.
33. Kaichev, V. V., G. Y. Popova, Y. A. Chesalov, A. A. Saraev, D. Y. Zemlyanov, S. A. Beloshapkin, et al. 2014. Selective oxidation of methanol to form dimethoxymethane and methyl formate over a monolayer V_2O_5/TiO_2 catalyst. J. Catal. 311:59–70.

34. Kim, D. S., Y. Kurusu, I. E. Wachs, F. D. Hardcastle, and K. Segawa. 1989. Physicochemical properties of MoO_3-TiO_2 prepared by an equilibrium adsorption method. J. Catal. 120:325–336.
35. Russell, A. S., and J. J. Stokes. 1946. Role of surface area in dehydrocyclization catalysis. Ind. Eng. Chem. 38:1071–1074.
36. Fransen, T., P. C. Van Berge, and P. Mars. 1976. Preparation of catalysts I – scientific bases for the preparation of heterogeneous catalysts. Proceedings of the First International Symposium held at the Solvay Research Centre, Elsevier.
37. Knoezinger, H., and H. Jeziorowski. 1978. Raman spectra of molybdenum oxide supported on the surface of aluminas. J. Phys. Chem. 82:2002–2005.
38. del Arco, M., S. R. G. Carrazán, C. Martín, I. Martín, V. Rives, and P. Malet. 1993. Surface dispersion of molybdena supported on silica, alumina and titania. J. Mater. Chem. 3:1313.
39. Ng, K. Y. S., and E. Gulari. 1985. Molybdena on titania I. Preparation and characterization by Raman and Fourier Transform Infrared spectroscopy. J. Catal. 92:340–354.
40. Brandhorst, M., S. Cristol, M. Capron, C. Dujardin, H. Vezin, G. Le bourdon, et al. 2006. Catalytic oxidation of methanol on Mo/Al_2O_3 catalyst: an EPR and Raman/infrared operando spectroscopies study. Catal. Today 113:34–39.
41. Payen, E., J. Grimblot, and S. Kasztelan. 1987. Study of oxidic and reduced alumina-supported molybdate and heptamolybdate species by in situ laser Raman spectroscopy. J. Phys. Chem. 91:6642–6648.
42. de Almeida, R. M., F. T. C. Souza, M. A. C. Júnior, N. J. A. Albuquerque, S. M. P. Meneghetti, and M. R. Meneghetti. 2014. Improvements in acidity for TiO_2 and SnO_2 via impregnation with MoO_3 for the esterification of fatty acids. Catal. Commun. 46: 179–182.
43. Shao, X., X. Zhang, W. Yu, Y. Wu, Y. Qin, Z. Sun, et al. 2012. Effects of surface acidities of MCM-41 modified with MoO_3 on adsorptive desulfurization of gasoline. Appl. Surf. Sci. 263:1–7.
44. Regalbuto, J. R., and J.-W. Ha. 1994. A corrected procedure and consistent interpretation for temperature programmed reduction of supported MoO_3. Catal. Lett. 29:189–207.
45. Chary, K. V. R., K. R. Reddy, C. P. Kumar, D. Naresh, V. V. Rao, and G. Mestl. 2004. Characterization and reactivity of molybdenum oxide catalysts supported on Nb_2O_5–TiO_2. J. Mol. Catal. A Chem. 223:363–369.
46. Ertl, G., H. Knözinger, and J. Weitkamp. 1999. Preparation of solid catalysts. WILEY-VCH Verlag GmbH, Weinheim, Germany.
47. Spivey, J. J., S. K. Agarwal, H. Knözinger, and E. Taglauer. 1993. Toward supported odxide catalysts via solid-solid wetting. Catalysis 10:1–40.
48. Sun, Q., J. Liu, J. Cai, Y. Fu, and J. Shen. 2009. Effect of silica on the selective oxidation of methanol to dimethoxymethane over vanadia–titania catalysts. Catal. Commun. 11:47–50.

Supporting Information

Additional Supporting Information may be found in the online version of this article:

Figure S1. Pore size distribution of the titania support.
Figure S2. A. Nitrogen adsorption/desorption isotherms and B. Pore size distribution for the catalysts prepared by wet impregnation.
Figure S3. XRD patterns for the catalysts prepared by incipient wetness impregnation.
Figure S4. IR-Raman spectra of the catalysts prepared by incipient wetness impregnation (full scale).
Figure S5. IR-Raman spectra of the catalysts prepared by incipient wetness impregnation (close up).
Figure S6. Carbon balance and product distribution over 8Mo(WI) as a function of temperature.

